

A multi-criteria methodology for effectiveness assessment of internal cylindrical grinding process with modified grinding wheels

Krzysztof Nadolny¹ · Abdulkareem Sh. Mahdi Al-Obaidi²

Received: 29 October 2015 / Accepted: 12 February 2016 / Published online: 27 February 2016
© The Author(s) 2016. This article is published with open access at Springerlink.com

Abstract One of the possible engineering solutions in developing grinding technology is modifying the structure of the grinding wheels. This solution is applicable and feasible for industrial conditions as it does not require interfering with the construction of the grinding machine. This article presents an important aspect of the development of new grinding wheels, which uses multiple criteria to evaluate their effectiveness in the grinding process. An analysis of previously used methods of grinding effectiveness evaluation was performed. A number of criteria for evaluating the most important expenditures and effects of these processes were highlighted. Next, a comparative evaluation of effectiveness of the six suggested grinding wheel modifications with sintered microcrystalline corundum grains and ceramic bond was performed. These grinding wheels were characterized by the following structural modifications: zone-diversified structure, modification of the bond microstructure, microdiscontinuities of the grinding wheel active surface, sandwich structure with a centrifugal system for provision of the coolant into the grinding zone as well as impregnated grinding wheel. Additionally, a grinding wheel whose structure was composed of a number of modifications was considered. The essential advantages and disadvantages

of the structural types of small-sized grinding wheels for peripheral grinding were determined. The results of the analysis of the effectiveness of the suggested solutions showed that it is possible to adjust the grinding wheel construction to the expected results of the given grinding operation as well as the technological conditions. It is also possible to combine these modifications in order to obtain additional synergetic effect of their positive influence on the grinding process.

Keywords Grinding effectiveness · Internal cylindrical grinding · Grinding wheel

Abbreviations

GF Grinding fluid
GWAS Grinding wheel active surface

1 Introduction

Due to its specific kinematics, the internal cylindrical grinding process is often described as one of the most difficult forms of machining using grinding wheels. Minor difference between grinding wheel and workpiece diameters results in a very long zone of contact between abrasive grains and ground surface. These conditions make internal cylindrical grinding extremely demanding for grinding wheels, especially in the context of their durability and operational time. The mechanical energy, introduced into the grinding process, resulted from the tool and the machined material's relative movement and is mostly transformed into heat [1, 2]. This causes a high thermal load for the grinding zone resulting from friction and deformation phenomena accompanying chip formation and material removal. This long contact zone between grinding wheel active surface (GWAS) and workpiece surface significantly hinders

✉ Krzysztof Nadolny
krzysztof.nadolny@tu.koszalin.pl

Abdulkareem Sh. Mahdi Al-Obaidi
abdulkareem.mahdi@taylor.edu.my

¹ Department of Production Engineering, Faculty of Mechanical Engineering, Koszalin University of Technology, Raclawicka 15-17, 75-620 Koszalin, Poland

² School of Engineering, Taylor's University, Taylor's Lakeside Campus, No. 1 Jalan Taylor's, 47500 Subang Jaya, Selangor DE, Malaysia

the effect of the grinding fluid. This is another factor impeding the heat dissipation from the grinding zone in the described process, which contributes to generation of grinding defects (undesired tensile residual stresses of workpiece surface layer, microfractures, grinding burns, etc.) [1, 2].

The long path of contact also leads to clogging of the GWAS by chips of the workpiece material, particularly when a process is conducted at a high material removal rate. This phenomenon results from the difficulty of transporting the grinding products (mainly chips) outside the grinding zone in the intergranular spaces of the GWAS. The clogging materials not only decrease the grinding wheel's cutting ability but they also increase friction and cause temperature increase in the process [3].

Another problem is the impeded provision of the grinding fluid (GF) into the grinding zone. The most frequently used cooling method does not guarantee even the provision of the GF whose effectiveness is constantly decreased as the grinding wheel moves into the opening. Because of the small size of the grinding wheel, it is not possible to use more advanced coolant provision techniques in such processes, e.g. the pressure method or using a "shoe" nozzle, as is done in case of surface grinding or external cylindrical grinding [4–6].

The literature can provide many examples of innovative grinding wheel design, for example, manufacturing the GWAS with defined grain pattern [7], introducing macro-discontinuities on the GWAS [8] or using pattered grinding wheels [9, 10]. These publications show that the design of abrasive tools is a crucial process from the point of view of efficiency as well as repeatability of the grinding process. The abrasive tool design for internal cylindrical processes should guarantee the following:

- Obtaining a multi-porous structure and simultaneously maintaining the required grinding wheel strength
- Even wear of the abrasive grains and the bond taking place in microvolumes
- Successful provision of the GF into the grinding zone during all stages of the process in order to obtain sufficient lubrication and cooling effects
- Effective transportation of chips and other grinding products (crushed grains) outside the grinding zone
- Decreasing the adhesion of chips to the GWAS in order to limit or eliminate the clogging phenomenon

One of the possible engineering solutions in the development of internal cylindrical grinding technology is modifying the grinding wheels' structure. Such modification usually does not require interfering with the construction of the grinding machine, which makes it feasible and applicable to industrial conditions. An important aspect of the development of new grinding wheels involves the evaluation of multiple criteria and their effectiveness in the grinding process.

Grinding effectiveness, defined in technological and economic terms, is understood as the relationship between the resulting machining effects and the expenditure required to achieve them. The results of are usually described by the following indirect parameters [1–3]:

- Grinding force
- Grinding power
- Absolute energy consumption
- Grinding temperature
- Vibrations of the machine-fixture-workpiece-tool system
- Acoustic emission
- Grinding capacity

and with the direct parameters such as the following:

- Surface roughness and waviness after grinding
- Residual stresses and microhardness of the workpiece surface layer
- Workpiece shape and dimensions
- Macro- and micro-wear of the grinding wheel
- Clogging of the grinding wheel active surface (GWAS)

In the case of the evaluation of abrasive machining effectiveness in relation to the grinding results, the crucial factors are the machined surface quality and the obtained material removal rate. The most important factors describing the expenditures are the grinding power and machining time that directly influence the process costs.

The aim of this work was to evaluate multi-criteria methodology for effective evaluation of the internal cylindrical grinding process carried out using grinding wheels with structural modifications. Such evaluation should be very useful in making modifications to a given grinding operation and its technological conditions.

2 Methodology for evaluation of internal cylindrical grinding with modified grinding wheels

Grinding effectiveness can be assessed using criteria divided into five groups. These are qualitative and performance indicators, grinding cost, grinding course, and associable indicators, also called synthetic indicators [1–3]. Table 1 presents indicators, from a survey of the literature, that have been frequently used for indirect quantitative grinding evaluation; they are divided into five groups.

It can be seen, from this survey, that there are two different ways of evaluating grinding wheel wear properties and the related grinding effectiveness. The first one concerns looking for new and original methods of evaluating grinding wheels' cutting capacity through, among others:

Table 1 Indices applied to the intermediate, quantitative evaluation of the grinding wheel cutting ability [1–3]

| Qualitative indicators | Performance indicators | Grinding costs indicators | Grinding course indicators | Synthetic indicators of grinding |
|--|--|--|--|---|
| $QI_1 = Ra, \mu m$ $QI_2 = \sigma, N/mm^2$ $QI_3 = \mu HV, N/mm^2$ $QI_4 = \Delta, \mu m$ | $PI_1 = Q_w, mm^3/s$ $PI_2 = Q_w/b_s, mm^3/s \cdot mm$ $PI_3 = j_p, pieces/s$ $PI_4 = v_{fr}, mm/s$ $PI_5 = v_{fr}/b_s, mm/s \cdot mm$ | $CI_1 = C_s/Q_w + C_g/(V_w/V_s) + C_d/\Delta V_w, \$/mm^3$ $CI_2 = f(C_f, C_v), \$/s$ | $GI_1 = F_n, N$ $GI_2 = F_n/b_s, N/mm$ $GI_3 = P_c, kW$ $GI_4 = P_c/b_s, kW/mm$ $GI_5 = \Theta, K$ $GI_6 = a_e, \mu m$ $GI_7 = F_n/A_D, N/mm^2$ $GI_8 = F_{ng}/A_{Dz}, N/mm^2$ $GI_9 = \lambda = \frac{e^{-\ln \frac{Q_w / F_n}{Q_w / F_n}}}{t_2 - t_1}, s^{-1}$ | $SI_1 = G = V_w/V_s, mm^3/mm^3$ $SI_2 = V_w/V_w, mm^3/mm^3$ $SI_3 = V_w/V_s \cdot P_c, W^{-1}$ $SI_4 = V_w/V_s \cdot P_c \cdot Ra, W^{-1} \cdot \mu m^{-1}$ $SI_5 = V_w \cdot F_n/V_s, N$ $SI_6 = f_r/F_n, mm/s \cdot N$ $SI_7 = Q_w/F_n, mm^3/s \cdot N$ $SI_8 = Q_w/P_c, mm^3/s \cdot W$ $SI_9 = V_w/F_n \cdot \lambda, mm^3/N$ $SI_{10} = V_w/F_n \cdot \lambda \cdot \Theta, mm^3/N \cdot K$ $SI_{11} = V_w^2/V_s \cdot F_n, mm^3/N$ $SI_{12} = 1/F_p \cdot Ra, N^{-1} \cdot \mu m^{-2}$ |

- Measuring the magnetic field of the grinding wheel active surface with a tendency to clogging [11]
- Measuring the acoustic pressure of the machine tool noise measure in the grinding zone and changes of the workpiece surface layer quality as a result of the “chatter” phenomenon
- Evaluation of the GWAS abrasive wear level on the basis of a photometric measurement of the average intensity of light reflected from the GWAS towards components of specular reflection, directed towards it in the form of a parallel beam into the area much larger than the size of an abrasive grain
- Measurement of the difference in temperatures in specific cross-sections of the grinding zone [12, 13]
- Determination of the value of factors connected with friction work in its different forms (sliding friction and friction connected with plastic deformations and friction of chips against the bond, as well as the bond against the machined material) on the basis of the GWAS stereometric parameters [14]
- Measuring the GWAS clogging intensity using a special device registering the frequency of rectangular impulses changing over the function of metal mass stuck to the grinding wheel surface

The second approach results from the desire to determine a generally acceptable recommended group of indicators. Unfortunately, attempts at unification of the grinding results evaluation methods have not led to the creation of a set of indicators that would be widely accepted and used.

It may be assumed that the most universal and most often applied grinding wheel cutting performance indicators (which are closely related to grinding effectiveness) are those that have been normalized. From the group presented in Table 1, the following indicators were defined as norms:

- $QI_1 = Ra, \mu m$ —arithmetic mean deviation of the workpiece roughness profile

- $QI_3 = \mu HV, N/mm^2$ microhardness in Vickers’ scale
- $PI_1 = Q_w, mm^3/s$ —material removal rate
- $PI_4 = v_{fr}, mm/s$ —radial table feed speed
- $GI_1 = F_n, N$ —the normal component of the grinding force
- $GI_3 = P_c, kW$ —grinding power
- $SI_1 = G = V_w/V_s, mm^3/mm^3$ —grinding indicator

Adopting the suggested evaluation criteria classification (Table 1), it may be assumed that one of the categories should be expressed quantitatively using at least one value, or a few values. It should be noted, however, that increasing the number of monitored signals is not always possible due to the limited number of sensors. In this study, it was decided that indicators connected with grinding costs would be omitted because of the difficulty in estimating the particular production cost components (specific to individual plant) and because they are only valid during a given period of time.

The selection of the normalized indicators shows that the machined surface quality may be evaluated with microhardness and arithmetic mean deviation of the workpiece roughness profile. It must be noted, however, that the majority of publications evaluate the workpiece surface quality obtained as a result of grinding processes, in terms of Ra , with information concerning microhardness treated as of secondary importance.

The evaluation of the process efficiency can be performed on the basis of the material removal rate, Q_w , or in the case of grinding processes with radial table feed through the speed of this movement v_{fr} . The course of the process is described by the normal component of the grinding force F_n and the grinding power P_c . For the purpose of comparing modifications in the grinding wheel construction, the material removal rate V_w was taken into consideration. This rate measures the period of grinding wheel life, as well as indicators describing the grinding wheel active surface condition such as the maximum roundness deviation Δ and surface share of clogging on the GWAS, A_c .

The group of synthetic indicators involved in grinding wheel effectiveness assessment included grinding indicator G and the synthetic index of single abrasive grain material removal rate SI_Q :

$$SI_Q = \frac{Q_{wcor} \cdot v_w}{N_{kin} \cdot \pi \cdot d_s \cdot T \cdot v_s} \mu\text{m}^3/\text{s}, \quad (1)$$

where:

| | |
|------------|---|
| Q_{wcor} | Corrected material removal rate, taking into consideration the prolongation of the real machining time caused by grinding wheel retardation, mm^3/s |
| b_s | Width of the grinding wheel measured parallel to the wheel axis, mm |
| d_s | External grinding wheel diameter, mm |
| N_{kin} | The number of kinetic cutting apexes per unit of the grinding wheel surface, mm^{-2} |
| v_s | Grinding wheel peripheral speed, m/s |
| v_w | Workpiece peripheral speed, m/s. |

It was also decided that this group of criteria should also include GF flow rate, Q_{GF} , as an indicator determining one of the ecological aspects of the grinding process resulting from the necessity of utilization of machining fluids.

The final selection of criteria, used to assess the effectiveness of grinding with modified grinding wheels, include the following indicators from five groups:

- Qualitative: Ra
- Efficiency: Q_w
- Grinding course: $\Delta P, V_w, \Delta, A$
- Ecological: Q_{GF}
- Synthetic ones: G, SI_Q

3 Characteristics of the assessed innovative grinding wheel structural modifications

The effectiveness of the internal cylindrical grinding process using grinding wheels possessing innovative structural modifications, expressed using a group of nine indicators, was compared with the results obtained using reference grinding wheels. Table 2 includes characteristics of six modified grinding wheels with a description of the reference grinding wheels to which were used for comparison with specific modifications.

4 Evaluation results of the effectiveness of internal cylindrical grinding with modified grinding wheels

Table 3 presents a comparison of absolute values with reference to the effectiveness evaluation indicators determined for grinding wheels with innovative modifications and values pertaining to reference grinding wheels. The values of the effectiveness evaluation indicators were calculated from the results of experimental tests of the grinding process. Table 4 presents a summary of the main parameters for the grinding experiments for each type of grinding wheel structural modification. The number of the indicators determined varied depending on the particular modifications and was selected so as to include the most important features of the evaluated solution.

In order to illustrate the influence of the given grinding wheel construction modification on the selected effectiveness evaluation indicators, radial charts of values expressed in percentages were created and are presented in Fig. 1. In these charts, fragments of lines connect data points. When the values of given effectiveness indicators were not determined, a broken line was drawn (these sections correspond to signs “–” in Table 3).

What can be selected on basis of the charts presented in Fig. 1 are those grinding wheel modifications which have the greatest influence on the given criterion of cylindrical grinding effectiveness evaluation. The introduction of zone-diversified structure of the grinding wheel (M1), GF provision system (M4), impregnation of the grinding wheel with graphite (M5), and integration of the modifications (M6) makes it possible to limit the machined surface roughness from between 21 and 35 %. Modification of the bond microstructure (M2) and the GWAS microdiscontinuities (M3), on the other hand, causes an increase of this criterion by 26 to 83 % (Fig. 1a).

In order to achieve the most reliable determination of the influence of the grinding wheel modification, grinding with reference grinding wheels was carried out with the same machining parameters. As a result of such an experimental test methodology, it was impossible to determine the influence of the examined modifications on the grinding material removal rate (Fig. 1b).

During analysis of changes in the grinding power, it was observed that the most meaningful decrease in this indicator (by 66 %) is possible in the case of modification integration (M6 on Fig. 1c). Approximately 20–30 % increase in the ΔP value, in comparison with the reference grinding wheel, was observed for the grinding wheel with microdiscontinuities (M3) and the grinding wheel impregnated with graphite (M5). In the case of the remaining grinding wheel structural modifications (M1, M2, and M4), their influence on this parameter was minor (Fig. 1c).

Values of the machined material removal rate V_w (Fig. 1d) make it possible to assess the given grinding wheel life period, which was determined for grinding wheels with modified bond (M2) and with GWAS microdiscontinuities (M3).

Table 2 Characteristics of the modified and reference grinding wheels against which efficiency was assessed

| Modified grinding wheel | | | | Reference grinding wheel (description and designation) |
|-------------------------|---|---|--|---|
| Modification code | Modification name and the grinding process in which the grinding wheel has been tested | Details of construction and designation | Construction scheme or microscopic SEM image | |
| M1 | <p>Zone-diversified structure</p> <p>Single-pass (traverse) grinding of 100Cr6 steel</p> <p>[15, 16]</p> | <p>The proportionate height of rough grinding b_{s1} and finish grinding b_{s2} zone: $b_{s1}/b_{s2} = 70\%/30\%$</p> <p>Parameters of conic chamfer: $\chi = 0.91^\circ$ $b = 12.6 \text{ mm}$</p> <p>Technical designation: 1-35×20×10-SG/F46K7VDG70% / SG/F80I7VDG30%</p> | | <p>Description: grinding wheel without zone-diversified structure, with conic chamfer enabling single-pass (traverse) grinding</p> <p>Parameters of conic chamfer: $\chi = 0.91^\circ$ $b = 12.6 \text{ mm}$</p> <p>Technical designation: 1-35×20×10-SG/F46K7VDG100%</p> |
| M2 | <p>Modification of the ceramic bond microstructure</p> <p>Plunge grinding with oscillations of 100Cr6 steel</p> <p>[17, 18]</p> | <p>Bond: glass-crystalline</p> <p>Bond structure: polymicrocrystalline-amorphous</p> <p>Type of crystalline phase: gahnit and willemite</p> <p>Technical designation: 1-35×10×10-SG/F46G10VTO</p> | | <p>Bond: glass</p> <p>Bond structure: amorphous</p> <p>Technical designation: 1-35×10×10-SG/F46G10V</p> |
| M3 | <p>Micro-discontinuities of the GWAS</p> <p>Single-pass (traverse) grinding of 100Cr6 steel</p> <p>[19]</p> | <p>Parameters of microdiscontinuities: $L_R = 6.43 \text{ mm}$ $t_{cir} = 9.38 \text{ mm}$ $t_{ax} = 0.23 \text{ mm}$ $b_R = 1.72 \text{ mm}$</p> <p>The relative area of microdiscontinuities on the GWAS: $A_R = 34.61\%$</p> <p>Technical designation: 1-35×20×10-SG/F46K7VDG70% / SG/F80I7VDG30%</p> | | <p>Description: grinding wheel with zone-diversified structure without micro-discontinuities of the GWAS</p> <p>Technical designation: 1-35×20×10-SG/F46K7VDG70% / SG/F80I7VDG30%</p> |

Table 2 (continued)

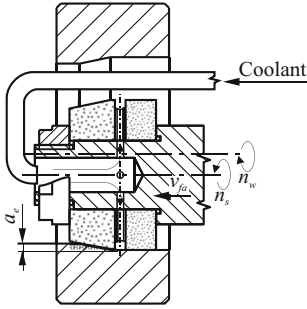
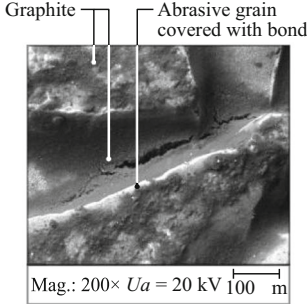
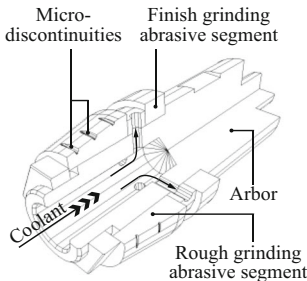
| Modified grinding wheel | | | | Reference grinding wheel (description and designation) |
|-------------------------|--|--|--|--|
| Modification code | Modification name and the grinding process in which the grinding wheel has been tested | Details of construction and designation | Construction scheme or microscopic SEM image | |
| M4 | Sandwich grinding wheel with a centrifugal system for provision of the coolant into the grinding zone Single-pass (traverse) grinding of 100Cr6 steel [20] | Description: divider with four channels of diameters $d_k = 3.0$ mm, for provision of the coolant directly into the grinding zone Technical designation: 1-35×20×10-SG/F46K7VDG70% / SG/F80I7VDG30% |  | Description: grinding wheel with zone-diversified structure without a centrifugal system of provision of the coolant into the grinding zone Technical designation: 1-35×20×10-SG/F46K7VDG70% / SG/F80I7VDG30% |
| M5 | Impregnated grinding wheel Reciprocal grinding of Titanium Grade 2® [21] | Impregnant: graphite Impregnation method: immersion in a solution of colloidal graphite powder Weight before impregnation: 17.22 g Weight after impregnation: 17.49 g Technical designation: 1-35×10×10-SG/F46G10VTO |  | Description: Nonimpregnated grinding wheel Technical designation: 1-35×10×10-SG/F46G10VTO |
| M6 | Integration of grinding wheel structural modifications Single-pass (traverse) grinding of 100Cr6 steel [22] | Integrated modification M1, M3 and M4 in one grinding wheel: – zone-diversified structure (M1) – micro-discontinuities shaped on active surface of the rough grinding zone (M3) – centrifugal system for provision of the coolant into the grinding zone (M4) Technical designation: 1-35×20×10-SG/F46K7VDG70% / SG/F80I7VDG30% |  | Description: grinding wheel without zone-diversified structure, with conic chamfer enabling single-pass (traverse) grinding Parameters of conic chamfer: $\chi = 0.91^\circ$ $b = 12.6$ mm Technical designation: 1-35×20×10-SG/F46K7VDG100% |

Table 3 The values of efficiency indicators of the grinding wheels with innovative modifications (M) and reference grinding wheels (R)

| Modification code | Efficiency indicators | | | | | | | | | | | | | | | | | |
|-------------------|-----------------------|-------|--------------------------------|----------------------|-----------------------|-----------------------|-----------|--------------------|-----------------|-----------------------------------|-------|------------|-------|-------|-----------|--------|--------|---|
| | Qualitative | | Performance | | | Grinding course | | | Grinding course | | | Ecological | | | Synthetic | | | |
| | $Ra, \mu\text{m}$ | | $Q_{gr}, \text{mm}^3/\text{s}$ | $\Delta P, \text{W}$ | V_{gr}, mm^3 | $\Delta, \mu\text{m}$ | $A_e, \%$ | Q_{gr}, L | $G, -$ | $SI_{gr}, \mu\text{m}^3/\text{s}$ | | | | | | | | |
| | R | M | R | M | R | M | R | M | R | M | R | M | R | M | R | M | R | M |
| M1 | 0.32 | 0.25 | 23.93 | 23.93 | 707.9 | 688.3 | - | - | - | - | - | 5.0 | 5.0 | - | - | 62,236 | 50,940 | |
| | 100 % | 76 % | 100 % | 100 % | 100 % | 97 % | - | - | - | - | - | 100 % | 100 % | - | - | 100 % | 82 % | |
| M2 | 0.30 | 0.38 | 7.14 | 7.14 | 382.6 | 356.8 | 46,400 | 46,400 | 47.28 | 32.50 | - | 4.0 | 4.0 | 102.1 | 69.5 | - | - | |
| | 100 % | 126 % | 100 % | 100 % | 100 % | 93 % | 100 % | 100 % | 100 % | 69 % | - | 100 % | 100 % | 100 % | 68 % | - | - | |
| M3 | 0.23 | 0.42 | 23.93 | 23.93 | 679.3 | 811.1 | 1364 | 4092 | - | - | - | 5.0 | 5.0 | - | - | 50,940 | 71,400 | |
| | 100 % | 183 % | 100 % | 100 % | 100 % | 119 % | 100 % | 300 % | - | - | - | 100 % | 100 % | - | - | 100 % | 140 % | |
| M4 | 0.31 | 0.20 | 17.92 | 17.92 | 723 | 673 | - | - | - | - | - | 5.0 | 1.0 | - | - | - | - | |
| | 100 % | 65 % | 100 % | 100 % | 100 % | 93 % | - | - | - | - | - | 100 % | 20 % | - | - | - | - | |
| M5 | 1.47 | 1.22 | 8.80 | 8.80 | 70 | 90 | - | - | - | - | 28.31 | 3.21 | 4.0 | 4.0 | - | - | - | |
| | 100 % | 83 % | 100 % | 100 % | 100 % | 129 % | - | - | - | - | 100 % | 11 % | 100 % | 100 % | - | - | - | |
| M6 | 0.33 | 0.26 | 17.92 | 17.92 | 832 | 370 | - | - | - | - | - | 5.0 | 1.0 | - | - | 48,970 | 56,175 | |
| | 100 % | 79 % | 100 % | 100 % | 100 % | 44 % | - | - | - | - | - | 100 % | 20 % | - | - | 100 % | 87 % | |

Table 4 Operational parameters of grinding experiments

| Grinding wheel modification code and name | Grinding process | Grinding parameters | |
|--|---|---|---|
| | | Grinding wheel with modifications | Reference grinding wheel |
| M1 Zone-diversified structure | Single-pass (traverse) grinding of 100Cr6 steel | $v_s = 60$ m/s $v_w = 0.75$ m/s $a_e = 0.20$ mm $v_{fa} = 2.0$ mm/s $Q_{GF} = 5.0$ L/min | $v_s = 60$ m/s $v_w = 0.75$ m/s $a_e = 0.20$ mm $v_{fa} = 2.0$ mm/s $Q_{GF} = 5.0$ L/min |
| M2 Modification of the ceramic bond microstructure | Plunge grinding with oscillations of 100Cr6 steel | $v_s = 60$ m/s $v_w = 1.5$ m/s $a_e = 0.20$ mm $v_{fa} = 20$ mm/s $v_{fr} = 0.2$ mm/min $Q_{GF} = 4.0$ L/min | $v_s = 60$ m/s $v_w = 1.5$ m/s $a_e = 0.20$ mm $v_{fa} = 20$ mm/s $v_{fr} = 0.2$ mm/min $Q_{GF} = 4.0$ L/min |
| M3 Micro-discontinuities of the GWAS | Single-pass (traverse) grinding of 100Cr6 steel | $v_s = 60$ m/s $v_w = 0.75$ m/s $a_e = 0.20$ mm $v_{fa} = 2.0$ mm/s $Q_{GF} = 5.0$ L/min | $v_s = 60$ m/s $v_w = 0.75$ m/s $a_e = 0.20$ mm $v_{fa} = 2.0$ mm/s $Q_{GF} = 5.0$ L/min |
| M4 Sandwich grinding wheel with a centrifugal system for provision of the coolant into the grinding zone | Single-pass (traverse) grinding of 100Cr6 steel | $v_s = 60$ m/s $v_w = 0.75$ m/s $a_e = 0.15$ mm $v_{fa} = 2.0$ mm/s $Q_{GF} = 5.0$ L/min | $v_s = 60$ m/s $v_w = 0.75$ m/s $a_e = 0.15$ mm $v_{fa} = 2.0$ mm/s $Q_{GF} = 1.0$ L/min |
| M5 Impregnated grinding wheel | Reciprocal grinding of Titanium Grade 2® | $v_s = 18$ m/s $v_w = 1.10$ m/s $a_e = 0.15$ mm $v_{fa} = 20$ mm/s $Q_{GF} = 4.0$ L/min | $v_s = 18$ m/s $v_w = 1.10$ m/s $a_e = 0.15$ mm $v_{fa} = 20$ mm/s $Q_{GF} = 4.0$ L/min |
| M6 Integration of grinding wheel structural modifications | Single-pass (traverse) grinding of 100Cr6 steel | $v_s = 60$ m/s $v_w = 0.60$ m/s $a_e = 0.20$ mm $v_{fa} = 1.5$ mm/s $Q_{GF} = 5.0$ L/min | $v_s = 60$ m/s $v_w = 0.60$ m/s $a_e = 0.20$ mm $v_{fa} = 1.5$ mm/s $Q_{GF} = 1.0$ L/min |

Grinding machine: universal grinding machine RUP 28P by Mechanical Works Tarnow SA, Poland, equipped with spindle type EV-70/70-2WB produced by Fisher, Switzerland (max. rpm 60,000 1/min, power of machine cutting 5.2 kW)

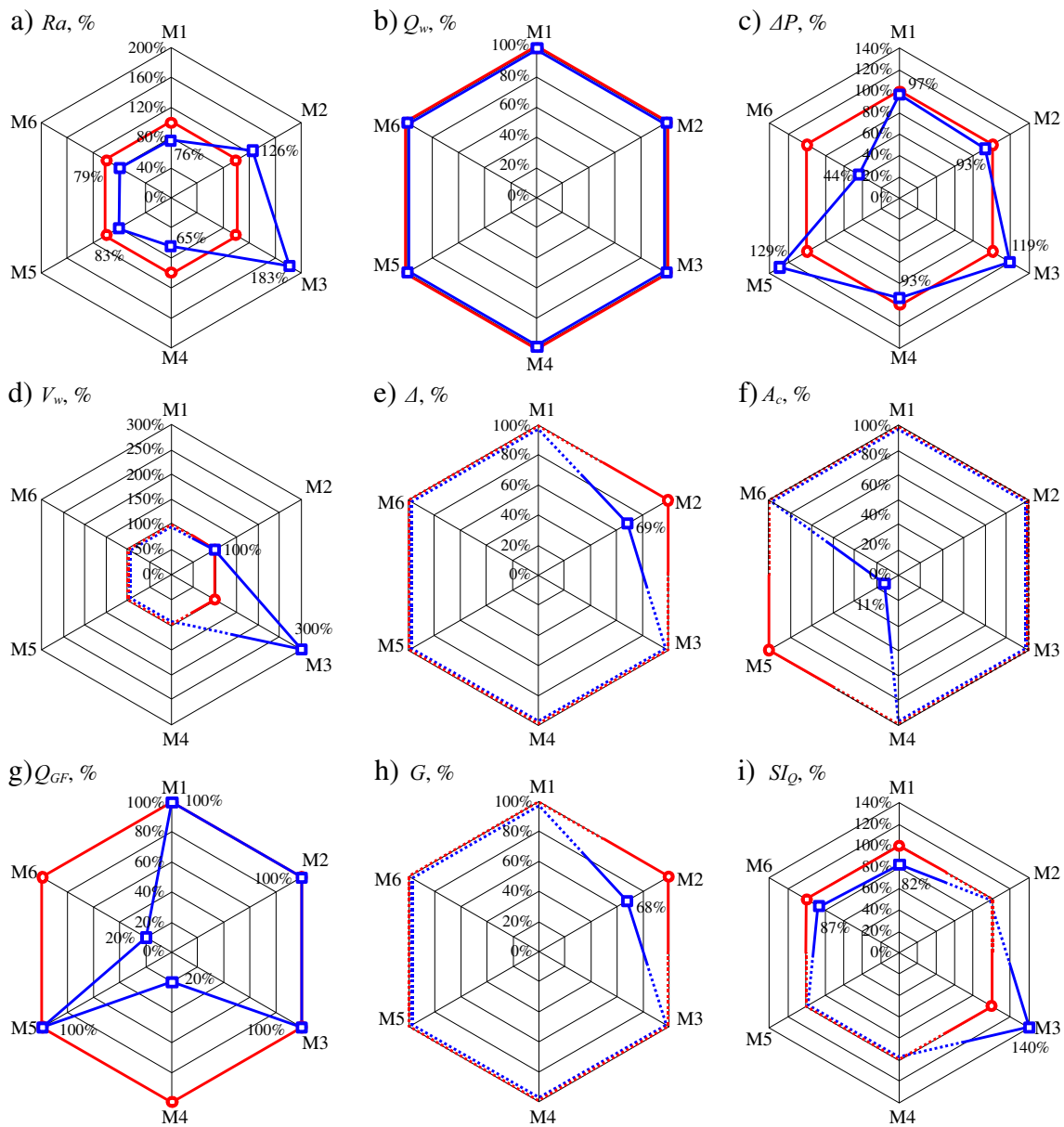
Dresser: single-grain diamond dresser $Q_d = 1.25$ kt

Dressing parameters: $n_{sd} = 12\ 000$ rpm, $v_{fd} = 10$ m/s, $a_d = 0.0125$ mm

Grinding fluid: 5 % water solution of Castrol Syntilo RHS oil

Application of the latter modification allowed for triple extension of the grinding wheel operating time in comparison with

the grinding wheel without GWAS microdiscontinuities (Fig. 1d).



M1 - Zone-diversified structure; M2- Modification of the bond microstructure; M3 - Micro-discontinuities of the GWAS; M4 - Sandwich grinding wheel with a centrifugal system of provision of the coolant into the grinding zone; M5 - Impregnated grinding wheel; M6 - Integration of grinding wheel structural modifications

○ Reference grinding wheel (100%)
 □ Modified grinding wheel

Fig. 1 The percentages of efficiency indicators for modified grinding wheels in relation to reference grinding wheels. **a** Arithmetic mean deviation of the workpiece roughness profile Ra . **b** Material removal rate Q_w . **c** Grinding power gain ΔP . **d** Material removal V_w .

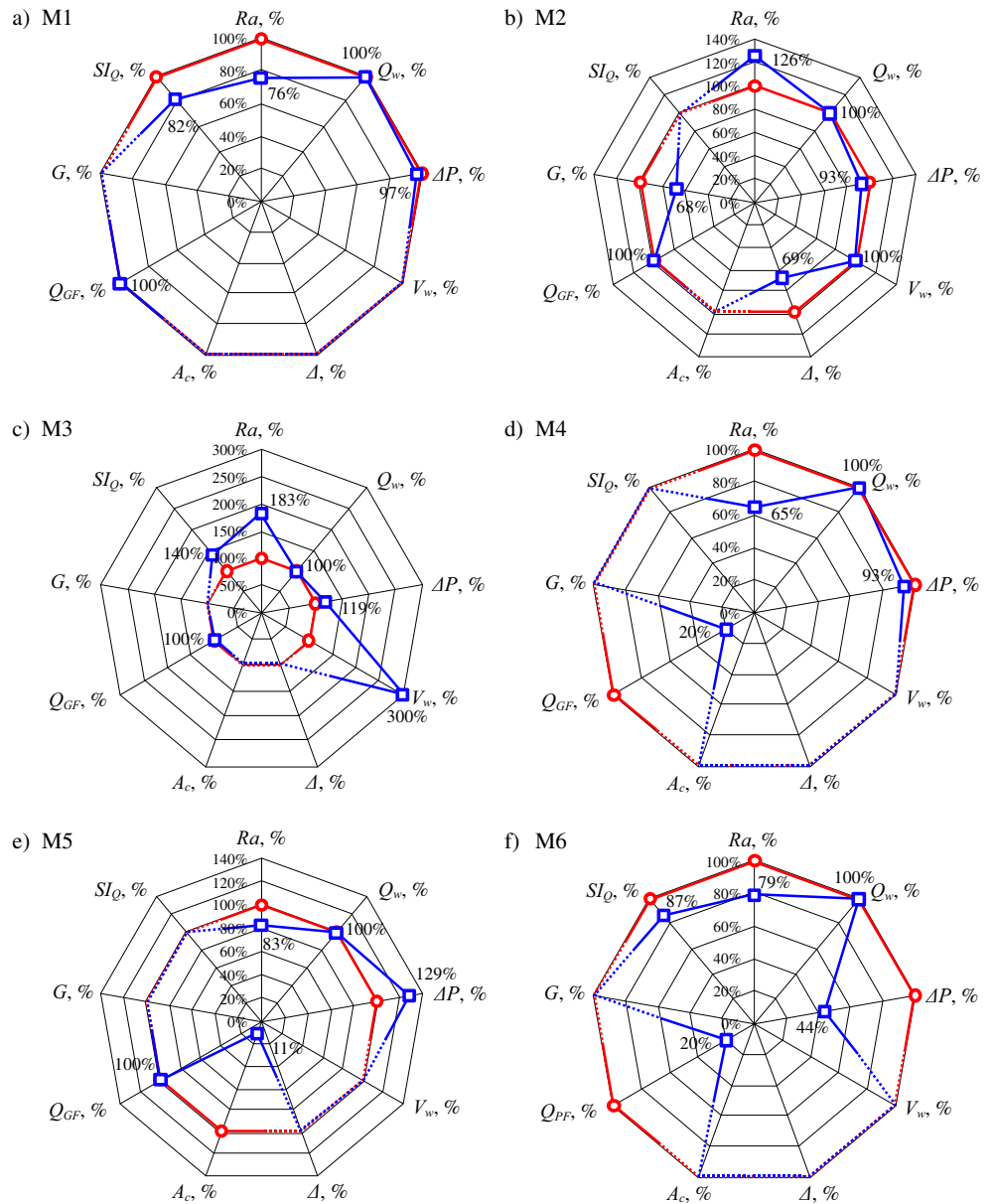
e Maximum roundness deviation of the GWAS Δ . **f** Surface share of the grinding wheel cloggings A_c . **g** Grinding fluid flow rate Q_{GF} . **h** Grinding index G . **i** Synthetic index of single abrasive grain material removal rate SI_Q

Changes in the grinding wheel roundness errors Δ in the period of its durability and volume wear of the grinding wheel V_s , necessary for the determination of the grinding indicator G , were registered only in case of grinding with grinding wheels that use a modified bond structure. Results of the evaluation of these two indicators (Δ and

G) made it possible to decrease the number of shape errors, with the application of bond modification, by 30 % (Fig. 1e), with a simultaneous proportional drop in the G indicator value (Fig. 1h).

Another indicator for the effectiveness of carrying out evaluations of modified grinding wheels referred to the share of

Fig. 2 Efficiency indicators of modified grinding wheels in relation to reference grinding wheels. **a** M1—zone-diversified structure. **b** M2—modification of the bond microstructure. **c** M3—microdiscontinuities of the GWAS. **d** M4—sandwich grinding wheel with a centrifugal system for provision of the coolant into the grinding zone. **e** M5—impregnated grinding wheel. **f** M6—integration of grinding wheel structural modifications



M1 - Zone-diversified structure;
 M2 - Modification of the bond microstructure;
 M3 - Micro-discontinuities of the GWAS;
 M4 - Sandwich grinding wheel with a centrifugal system of provision of the coolant into the grinding zone;
 M5 - Impregnated grinding wheel;
 M6 - Integration of grinding wheel structural modifications

—○— Reference grinding wheel (100%)
 —□— Modified grinding wheel

surface clogging on the GWAS A_c . This indicator was the most important in examinations of impregnated grinding wheels used during the processes of grinding hard-to-cut materials, for which reason its value was determined only in this case. A considerable (over 90 %) decrease of the share of GWAS clogging A_c with the machined material for the grinding wheel impregnated with graphite (M5 in Fig. 1h) was also found.

A comparison of the ecological indicator value Q_{GF} for the examined modifications showed the possibility of a definitive (fivefold) reduction of its value in the case of utilizing

grinding wheels with the system of internal GF provision to the grinding zone—modifications M4 and M6 in Fig. 1g.

In the case of the modification of the grinding wheel structure, for which it was possible to determine changes in material removal rate per single cutting apex SI_Q , the values of this indicator (Fig. 1i) corresponded to changes in the machined surface roughness expressed by Ra (Fig. 1a).

Figure 2 presents charts demonstrating percentile changes in the values of particular grinding effectiveness evaluation indicators, as determined for the six examined grinding wheel

structural modifications, and in relation to proper reference grinding wheels. This comparison makes it possible to evaluate the advantages and disadvantages of different applications of the given modification.

Zone-diversification of the grinding wheel structure (M1) applied in single-pass grinding allows for a 24 % decrease of machined surface roughness Ra and a minor decrease in the grinding power ΔP which does not influence material removal rate Q_w or coolant expenditure (Fig. 2a).

Modification of the ceramic bond microstructure exerts a positive influence on errors in grinding wheel shape Δ and grinding power ΔP , a neutral influence on material removal rate Q_w , durability V_w , and GF expenditure, and a negative influence on the machined surface roughness Ra and the grinding indicator G (Fig. 2b). This means that such modifications should be used in processes in which the grinding wheel is in operation for a lengthy period of time and require the smallest roundness errors possible, taking into consideration both an increase in volume wear and a deterioration in the quality of the machined surface in comparison with the reference grinding wheel.

Shaping GWAS microdiscontinuities caused an 83 % increase in the machined surface roughness and a 19 % increase in the grinding power. The values of these indicators were determined as an average of the grinding wheel's durability period, which in the case of the grinding wheel with microdiscontinuities was three times longer (Fig. 2c).

Application of the system of internal GF provision into the grinding zone did not influence the material removal rate Q_w , but it did have a positive influence on the machined surface roughness (Ra parameter lowered by 35 %), the grinding power (ΔP lowered by 7 %), and the grinding fluid expenditure (Q_{GF} lowered by 80 %) in comparison with the reference grinding wheel (Fig. 2d).

The most important reason for impregnating the grinding wheel with graphite was the limitation of the phenomenon of GWAS clogging with ground products, mostly machined material chips. As the comparison of effectiveness evaluation indicators for this modification shows (Fig. 2e), an 89 % drop in the surface share of clogging on the GWAS A_c was observed, with a simultaneous 17 % decrease of the machined surface roughness described by parameter Ra and a 29 % increase in the grinding power ΔP .

The last of the charts presented in Fig. 2 refers to the integration of three modifications in one grinding wheel (Fig. 2f). The percentage values of the effectiveness indicators showed a fivefold decrease in the GF expenditure, a decrease of the grinding power by 66 %, and a decrease in the machined surface roughness by 21 %, all the while maintaining a level of material removal rate Q_w in comparison with the reference grinding wheel.

5 Conclusions

The multi-criteria methodology applied to the assessment of the effectiveness of grinding process with grinding wheels utilizing innovative structural modifications was compared to results obtained for reference grinding wheels—free from modifications. The values of the effectiveness indicators made it possible to examine particular solutions and indicate their strengths and weaknesses. The most important advantages of the assessed modifications include the following:

- Decreasing the surface roughness after grinding, expressed by the parameter Ra within the range of 17 to 35 % (modifications M1, M4, M5, M6).
- Limitation of the grinding power increase ΔP from 3 to 66 % (modifications M1, M2, M4, M6).
- A threefold prolongation of the grinding wheel life, expressed with material removal V_w , in the case of the application of GWAS microdiscontinuities (modification M3).
- About 30 % limitation of the grinding wheel roundness error value Δ in the case of the application of a modified bond microstructure is possible to obtain using modification M2.
- Decreasing the intensity in the creation of cloggings on the GWAS during the processes associated with grinding hard-to-cut materials, expressed by an 89 % reduction of the surface share of the cloggings A_c in the case of the application of grinding wheels impregnated with graphite (modification M5).
- The possibility of achieving positive ecological results through a fivefold decrease in the GF expenditure Q_{GF} , in the case of the application of the system of internal grinding fluid provision (modifications M3 and M6).

Apart from the positive aspects of their application, the innovative grinding wheel structural modifications, described here, are also characterized by their negative influence upon some of the evaluated grinding process parameters. In particular, these are as follows:

- Deterioration of the machined surface roughness expressed by parameter Ra (between 23 and 83 %) in the case of the application of grinding wheels with modified ceramic bond microstructure and grinding wheels with GWAS microdiscontinuities (modifications M2 and M3)
- Increased grinding power ΔP by 19 % in the case of grinding using a grinding wheel with GWAS microdiscontinuities (M3) and by 29 % in the case of the application of a grinding wheel impregnated with graphite (M5)

- A 32 % decrease of the grinding parameter G in the process of grinding carried out using a grinding wheel with modified ceramic bond microstructure (M2)

A wide variety of suggested solutions makes it possible to adjust modifications to the given grinding operation and technological conditions. It is also possible to combine modifications in order to obtain the additional synergetic effect of their positive influence on the process of internal cylindrical grinding with sintered microcrystalline corundum grains.

In future work, the authors will focus on solutions which enable minimizing or eliminating the indicated disadvantages of selected grinding wheel structural modifications. There is a wide range of options for future improvement of described modifications, particularly in the case of the microstructure of ceramic bond (changes in the share and type of the crystalline phases), impregnated grinding wheels (changes in the type of impregnate, the degree of pore filling by impregnation) as well as microdiscontinuities of the GWAS (changes in the share, orientation, and shape of microdiscontinuities).

6 Nomenclature

| | |
|------------|---|
| A_c | Surface share of the grinding wheel cloggings on the grinding wheel active surface, % |
| A_D | Cross-section of cutting layer, mm^2 |
| a_e | Machining allowance (working engagement), μm |
| a_d | Dressing allowance, mm |
| b_s | Width of the grinding wheel measured parallel to the wheel axis, mm |
| C_d | Costs of a single dressing cycle, \$ |
| C_f | Fixed costs, \$ |
| C_g | Costs of grinding wheel, $\$/\text{mm}^3$ |
| C_s | costs of grinding machine servicing, \$ |
| C_v | Variable costs, \$ |
| d_s | External grinding wheel diameter, mm |
| F_c | Cutting force, N |
| F_n | Normal component of the cutting force, N |
| F_{ng} | Normal component of the cutting force per single abrasive grain, N |
| f_r | Radial table feed, mm |
| G | Grinding indicator ($G = V_w/V_s$), mm^3/mm^3 |
| j_p | Number of completed workpieces |
| N_{kin} | The number of kinetic cutting apexes per unit of the grinding wheel surface, mm^{-2} |
| n_{sd} | Grinding wheel rotational speed while dressing, rpm |
| P_c | Cutting/grinding power, W |
| Q_d | Diamond dresser mass, kt |
| Q_{GF} | Grinding fluid flow rate, L/min |
| Q_w | Material removal rate, mm^3/s |
| Q_{wcor} | Corrected material removal rate, taking into consideration the prolongation of the real machining |

| | |
|----------|--|
| | time caused by grinding wheel retardation, mm^3/s |
| Ra | Arithmetic mean deviation of the workpiece roughness profile, μm |
| SI_Q | Synthetic index of single abrasive grain material removal rate, $\mu\text{m}^3/\text{s}$ |
| V_s | Grinding wheel volumetric wear, mm^3 |
| V_w | Material removal, mm^3 |
| v_{fa} | Axial table feed speed while grinding, mm/s |
| v_{fd} | Axial table feed speed while dressing, mm/s |
| v_{fr} | Radial table feed speed, mm/s |
| v_s | Grinding wheel peripheral speed, m/s |
| v_w | Workpiece peripheral speed, m/s |

Greek symbols

| | |
|----------------|--|
| σ | Stresses in the workpiece surface layer, N/mm^2 |
| Δ | Maximum roundness deviation of the grinding wheel, μm |
| ΔP | Grinding power gain |
| λ | Factor characterizing the intensity of changes in the grinding wheel cutting ability |
| μHV | Microhardness of the workpiece surface layer in Vickers' scale, N/mm^2 |
| Θ_p | Grinding temperature, K |

Acknowledgments The authors would like to thank Prof. David Hukins for his kind assistance in checking the English language of this paper.

Compliance with ethical standards

Conflict of interest The authors declare that they have no conflict of interest.

Funding This study did not receive any grant funding.

Open Access This article is distributed under the terms of the Creative Commons Attribution 4.0 International License (<http://creativecommons.org/licenses/by/4.0/>), which permits unrestricted use, distribution, and reproduction in any medium, provided you give appropriate credit to the original author(s) and the source, provide a link to the Creative Commons license, and indicate if changes were made.

References

1. Klocke F (2009) Manufacturing processes 2: grinding, honing, lapping. Springer-Verlag, Berlin
2. Marinescu ID, Hitchiner M, Uhlmann E, Rowe WB, Inasaki I (2007) Handbook of machining with grinding wheels. CRC Press, Boca Raton
3. Jackson MJ, Davim JP (2010) Machining with abrasives. Springer, New York
4. Brinksmeier E, Heinzl C, Wittmann M (1999) Friction, cooling and lubrication in grinding. CIRP Ann-Manuf Technol 48:581–598

5. Nguyen T, Zhang LC (2009) Performance of a new segmented grinding wheel system. *Int J Mach Tool Manu* 49: 291–296
6. Tawakoli T, Hadad M, Sadeghi MH, Daneshi A, Sadeghi B (2011) Minimum quantity lubrication in grinding: effects of abrasive and coolant–lubricant types. *J Clean Prod* 19:2088–2099
7. Aurich JC, Herzenstiel P, Sudermann H, Magg T (2008) High-performance dry grinding using a grinding wheel with a defined grain pattern. *CIRP Ann-Manuf Techn* 57:357–362
8. Kirsch B, Aurich JC (2014) Influence of the macro-topography of grinding wheels on the cooling efficiency and the surface integrity. *Procedia CIRP* 13:8–12
9. Oliveira JFG, Bottene AC, Franca TV (2010) A novel dressing technique for texturing of ground surfaces. *CIRP Ann-Manuf Techn* 59:361–364
10. Silva EJ, Oliveira JFG, Salles BB, Cardoso RS, Reis VRA (2013) Strategies for production of parts textured by grinding using patterned wheels. *CIRP Ann-Manuf Techn* 62:355–358
11. König W, Lauer-Schmalt H (1978) Loading of the grinding wheel phenomenon and measurement. *CIRP Ann-Manuf Techn* 27:217–220
12. Tawakoli T (1990) High-performance surface grinding, technology process planning and economic use. VDI-Verlag GmbH, Dusseldorf [in German]
13. Tawakoli T (1992) High efficiency deep grinding (HEDG) of inconel and other materials. *VDI-Z Integrierte Produktion* 134: 48–57 [in German]
14. Dabrowski L, Marciniak M, Oczos KE (2002) Cutting surface of the grinding wheel as a component of tribological system. *Arch Civ Mech Eng* 2:47–58
15. Herman D, Plichta J, Nadolny K (2006) New ceramic abrasive tools for rough and finishing grinding in one pass. *Mater Sci Forum* 526: 163–168
16. Nadolny K, Kaplonek W (2012) Design of a device for precision shaping of the grinding wheel macro- and microgeometry. *J Cent South Univ T* 19(1):135–143
17. Herman D (1998) Glass and glass-ceramic binder obtained from waste material for binding alundum abrasive grains into grinding wheels. *Ceram Int* 24(7):515–520
18. Herman D, Markul J (2004) Influence of microstructures of binder and abrasive grain on selected operational properties of ceramic grinding wheels made of alumina. *Int J Mach Tool Manu* 44:511–522
19. Nadolny K (2013) Microdiscontinuities of the grinding wheel and their effects on its durability during internal cylindrical grinding. *Mach Sci Technol* 17(1):74–92
20. Nadolny K (2015) Small-dimensional sandwich grinding wheels with a centrifugal coolant provision system for traverse internal cylindrical grinding of steel 100Cr6. *J Clean Prod* 93:354–363
21. Sienicki W, Wojtewicz M, Nadolny K (2011). Method of modifying ceramic abrasive tools by impregnation. Polish patent application No. P. 395441
22. Nadolny K (2012) The effect of integrating the structural modifications of the grinding wheel upon the internal cylindrical grinding process. *Arch Civ Mech Eng* 12(1):60–67